ANNALI DI GEOFISICA, VOL. XXXVI, N. 1, April 1993

The influence of source complexity on the polarization and azimuthal radiation of *S*-waves, and a simplified synthesis of the macroseismic field

Livio Sirovich([1])([*]) **and Claudio Chiaruttini**([2])
([1]) *Osservatorio Geofisico Sperimentale, Trieste, Italia*
([2]) *Istituto di Geodesia e Geofisica, Università di Trieste, Italia*

Abstract
An analysis of *S*-wave polarization evidenced that the rupture of the 0s sub-event propagated towards the NW; horizontal PGAs originated from the source segments closest to each station; in Sturno, small-scale ruptures on the edge of an unbroken barrier produced the strongest horizontal PGA recorded during the whole event; the broken parts of the fault continued to radiate after the passage of the rupture front. In this case, the seismic-energy radiation in different azimuths was significatively controlled by the focal mechanism and by the length of the source. A simple algorithm to synthesize the intensity field from the gross features of the source is used and the results obtained are compared with experimental observation.

1. Introduction

Regional seismic-hazard studies require integrating information on the effective energy radiation contained in instrumental records and in historical seismic catalogues. The most common way to use accelerograms is based on attenuation laws of strong-motion peak values. In dealing with historical information, one is faced with various kinds of intensity attenuations. An aspect of the radiation field that is usually not taken into account is the lobed shape of the isoseismals. The approximation of isolines by circles or ellipses is an inadequate procedure, especially when damaging earthquakes show similar patterns repeating over time. For three centuries at least, this has happened in the southern Apennines: the 1980 earthquake appears to be the most recent of a repetitive series. The study of instrumental records and the comparison of the macroseismic effects of past and present events will contribute to a better understanding of seismic-energy release in the area and to a more complete use of all available information. From this perspective, the aim of the work is to understand how basic features of the strong-motion field of the Irpinia 1980 earthquake are related to basic source features. If so, there is an opportunity to model the strong-motion field of some historical earthquakes in the area.

In detail, we will consider the following points:

- analysing some features of *S*-waves polarization;
- understanding the seismic-energy radiation in different azimuths;
- identifying the major parameters that control the distribution of strong-motion peak values; the influence of gross source features like dimension, focal mechanism, and directivity, is particularly addressed;
- assessing the influence of the above parameters on the isoseismals' shape;
- providing a simple algorithm to synthesize the intensity field and, inversely, to infer information about gross features of historical earthquakes from macroseismic observations.

There is a general agreement that this complex event consisted of three main rupture episodes, at 0s, 19s and 39s from the nucleation origin time. This work deals primarily with the first sub-

event, the strongest one; the second will be also considered.

2. The data set

The accelerograms were recorded by the ENEA and ENEL Joint Commission. PGA values were obtained from hodogram plots of each pair of digitized horizontal components (scanning lag: 0.00244s) after removing the mean over 5s time windows. All recording stations lie on the free-field; with the exception of MER, all are on stiff or hard grounds (Faitelli, 1978). The influence of site topography is thought to be irrelevant (perhaps with the exception of CAL). Thus it is possible to investigate the polarization and the variability of PGA with limited site disturbances.

3. Polarization analyses

We have used hodograms to investigate wave polarization. In the low-frequency band, they carry information on gross features of the source; details can be seen in the high frequencies.

S_H and S_V waves do not compose linearly (Nuttli and Whitmore, 1962); nevertheless, when proper conditions are satisfied, hodograms carry information on the direction of incoming waves. Our argument is twofold (as discussed in: Siro and Chiaruttini, 1991). First, the S_H or the S_V component is often much larger than the other; this reduces the discrepancy between hodogram orientation and ray direction. Phase shifts can further decrease the discrepancy.

Second, usually both hard rocks and superficial soft layers are transversely isotropic owing to stratification, cleavage, etc. If the time delay caused by this anisotropy exceeds several periods, S_H or S_V split waves compose with random waves; if only the most prominent arrivals of energy are considered, their polarization will not be significantly altered. It seems (Siro and Chiaruttini, 1991) that in the case of the studied earthquake such a splitting effect is plausible.

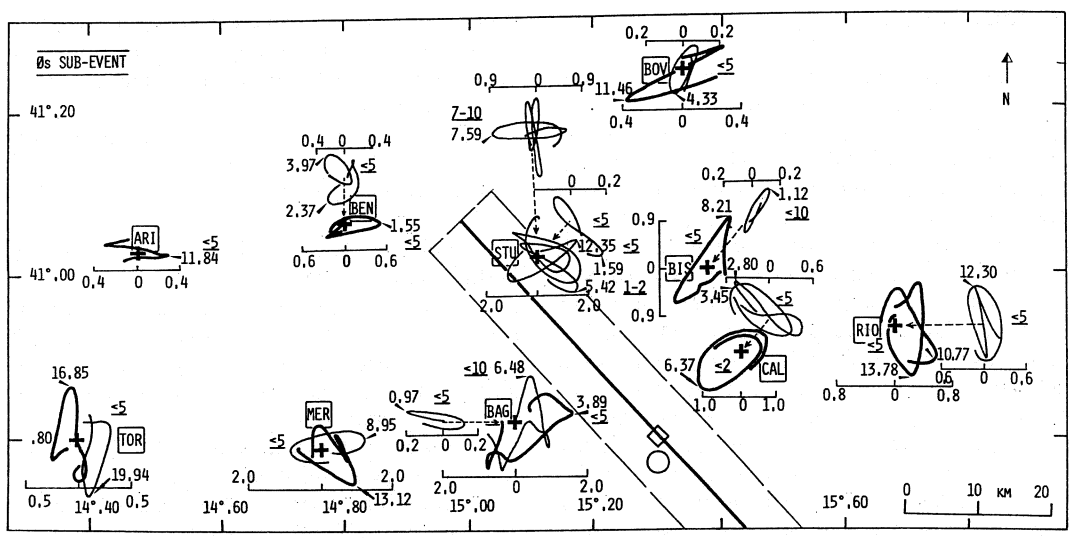

Fig. 1. Hodogram plots of the 0 s sub-event. The oblique stripe includes epicenters of aftershocks from 23 November to 3 December 1980 (Scarpa and Slejko, 1982). The square and the circle are respectively the epicenters of the first break as determined by Scarpa and Slejko (1982) and by Deschamps and King (1983). Heavy crosses show the geographical position of the recording stations. Heavy lines in the hodogram plots refer to lobes carrying the absolute maximum accelerations inside the record of each station during this sub-event; scales are in $g/10$, numbers with arrows indicate the relative time (s) of each shown phase inside the record of each station. Underlined numbers indicate the filtering adopted for each hodogram (under permission of BSSA).

Figure 1 shows polarizations of prominent arrivals of the 0s sub-event, including the maxima. Source-station geometry and timing place constraints on the wave type and direction. For example, at the beginning of the station BAG record, a pulse stands out at 0.97s. Since it is EW polarized, and given the station location and fault kinematics, it is mainly controlled by S_V waves. Later, the two maxima occur at 3.89 and 6.48s. They are also attributed to prevailing S_V waves. In conclusion, three consecutive pulses reach BAG from ESE, NE and NNE. The results of this analysis are shown in fig. 2. All hodograms consistently suggest that the 0s rupture propagated towards NW.

The highest amplitude phases were generally radiated by the source segments closest to each station. An interesting case involves station STU, the nearest to the breaking fault but at some distance from the epicentre. Hodograms of low-passed horizontal records (fig. 3a) and 3b)) exhibit mainly S_H polarized energy from the S_V as the rupture passes by the station. In the higher frequencies (fig. 3c) and 3d)) a totally different pattern is present. We interpret it as completely split S_H and S_V energy coming from the south, as it is too early to come from the west. We argue that a stress concentration occurred on the edge of an unbroken barrier south of STU where a gap of aftershocks (see Deschamps and King, 1984) is also present. Small-scale ruptures produced the strongest acceleration recorded during the whole event. A more complete analysis of all three sub-events is given elsewhere (Siro and Chiaruttini, 1989).

Figures 3a) to 3d) also strongly suggest that the source remained active for several seconds after the passage of the rupture front. It is unlikely that lateral scattering would produce so strong and consistently oriented patterns.

4. Influence of source dimension and of focal mechanism on strong-motion

Analyzing data from a single earthquake allows one to investigate the effects of the source geometry and focal mechanism on strong-motion acceleration. For this purpose, we considered the initial 35s window of the records. We recall that at all triggered stations, with the exception of CAL, the peak acceleration occurred during the 0s or 19s sub-event. As mentioned before, there is evidence for a northwestward propagation of the rupture. There is also weaker evidence for a southeastward propagation of the 19s sub-event.

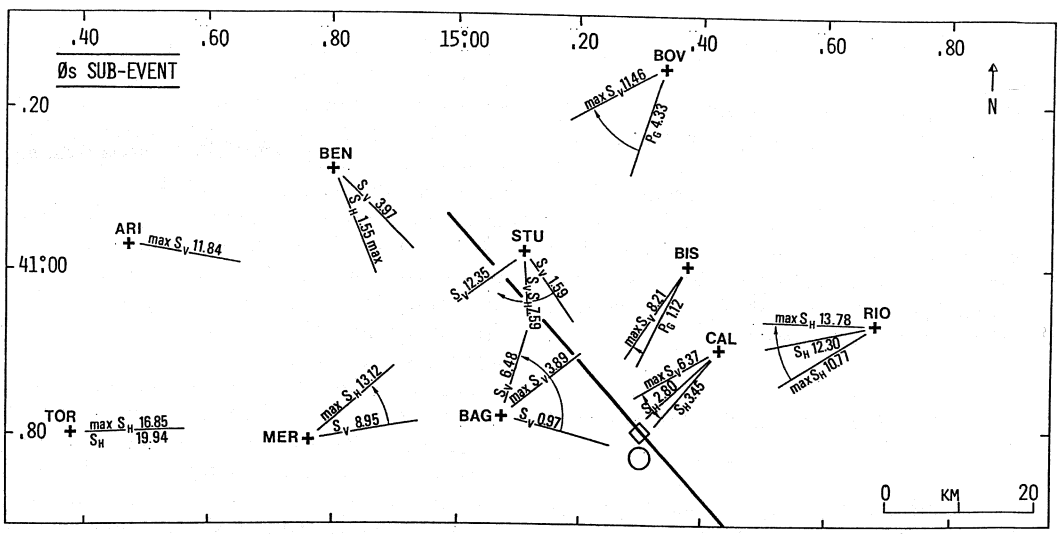

Fig. 2. The incoming directions of prominent phases in successive times indicate NW propagation of the 0 s sub-event. Type of wave and relative time are shown; other symbols as in fig. 1 (under permission of BSSA).

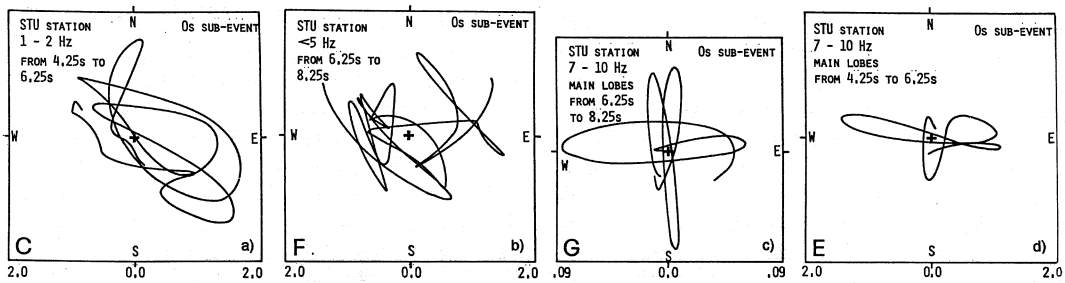

Fig. 3. Hodogram plots from station STU. a) 1 to 2 Hz pass-band, 4.25 to 6.25 time-window; S_H waves reach the station from the SSW, where the closest part of the rupture is (see also fig. 1). b) 5 Hz low-pass, 6.25 to 8.25 s time-window; mainly S_H lobes coming from the SW are seen. c) 7 to 10 Hz pass-band, same time-window as in fig. 3b). d) 7 to 10 Hz pass-band, same time-window as in fig. 3a). Strong high-frequency pulses come approximately from the south as S_H and S_V, most likely split, waves. Only the strongest lobes are shown (under permission of BSSA).

Table I. Summary of the regression analyses of log PGA with respect to log D.

	regression coefficients		st. error of	R	significance
	a	b	the estimate	squared	
D from epicenter	1.36	-0.86±0.31	0.24	0.41	0.009
D from hypocenter	1.80	-1.10±0.38	0.23	0.44	0.007
(*) H = 0 km	0.92	-0.68±0.21	0.22	0.50	0.003
(*) H = 10 km	1.24	-0.87±0.28	0.23	0.47	0.005

(*) D from the axis of epicenter distribution (see the text), at variable depth H.

Because of this, the directivity effect was also considered.

The aftershock epicenters are aligned along the Apenninic chain; however, the hypocenters do not lie on a plane. In such a complex situation and in view of the applicative purpose of the work, we approximate the source by the horizontal axis of the distribution of the first 10 days aftershocks (Scarpa and Slejko, 1982). Note that more detailed models are usually unavailable in the case of historical earthquakes.

5. Sources of dispersion in the experimental data

As a preliminary attempt to understand the features of the strong-motion field, we use the simple model:

$$\log \mathrm{PGA} = a + b \log D \qquad (1)$$

where PGA is given in $g/10$; a and b are regression coefficients and D is distance in km. Several definitions of D were used: distance from the epicenter, from the hypocenter, and from what we defined as the source; different source depths H have been tried. Table I shows that the distances from the line source are better estimators than point hypocentral and epicentral distances. The data and the regression line for the best result (H=0) are shown in fig. 4. The MER site is in parethesis because it is the only one with superficial cohesionless sediments.

Let us examine now the influence of the radiation pattern on data dispersion. Figure 5 shows the recorded PGAs corrected for the source distance by eq. (1). Although there is a lack of data towards the SW, it is easily seen that the ratios are not randomly distributed about unity; rather, they seem to follow a well-defined pattern, with significant minima at stations AUL and BEN, strong maxima at BRI and in the direction of

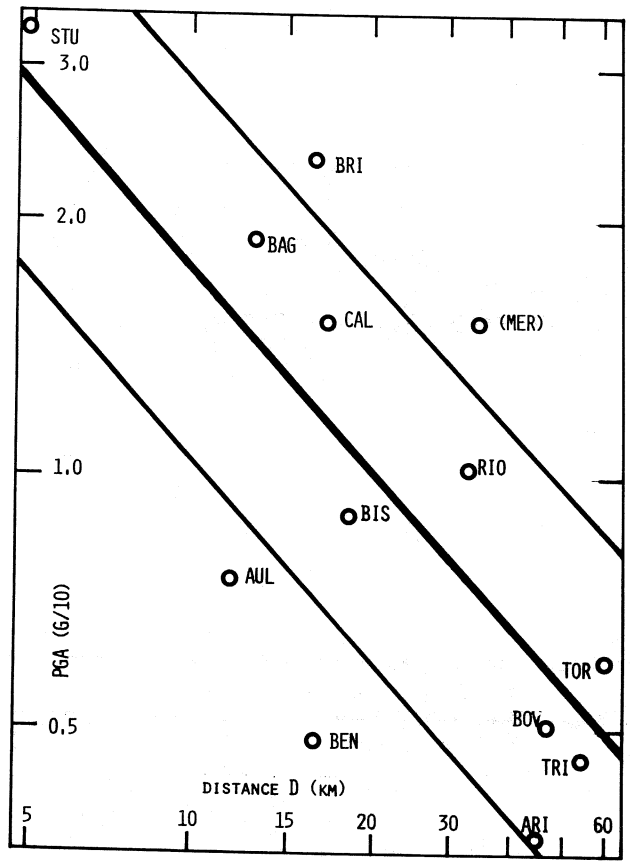

Fig. 4. Attenuation of PGA with distance from the horizontal projection of the assumed line source. Thin lines indicate the standard error of the estimate.

BAG, TOR (and MER). Furthermore, there is a smooth variation from STU to RIO and a relative minimum at TRI. There is a general consensus that the fault dips at about 60° towards NE and the strike is in the Apenninic direction (see Pantosti and Valensise, 1990, for a review). In this study we assume 318° for strike and 64° for dip as representative values. The slip direction is more controversial and normal faults with either a left-lateral or a right-lateral slip component have been proposed, the rake ranging from 318° (Deschamps and King, 1983) to 250° (Brüstle and Müller, 1983). Here we explore these alternatives considering the above two extreme cases and the pure normal fault (rake=270°). Both Westaway and Jackson (1987) and Pantosti and Valensise (1990) believe in a slight left-lateral component (respectively 5° and less than approximately 20°).

The radiation from a point source located at the hypocenter does not succeed in simulating the azimuthal distribution of the experimental values; figure 6 shows one of the unsuccessful trials.

If we assume instead that the maximum shaking is produced by radiation from the source point closest to each station, the patterns of fig. 7a) to 7c) are obtained. Of course, the appropriate azimuths and take-off angles were considered. All three mechanisms produce a wide lobe in the NE direction, which resembles that of fig. 5. From fig. 7c) it appears that some amount of left-lateral strike-slip is necessary to simulate all other features of fig. 5. This is a good example of the

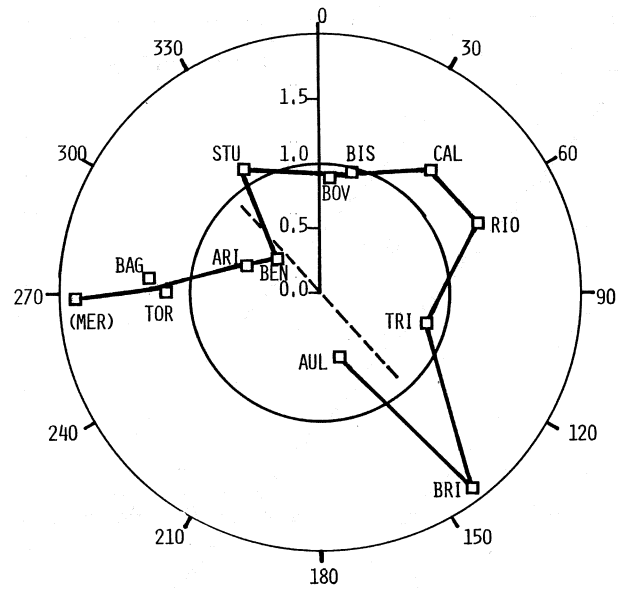

Fig. 5. Ratio of recorded PGA and acceleration predicted by the regression in fig. 4, as a function of the azimuth of the stations with respect to the epicenter. The circle is drawn at unit ratio; the dashed line indicates the strike of the fault.

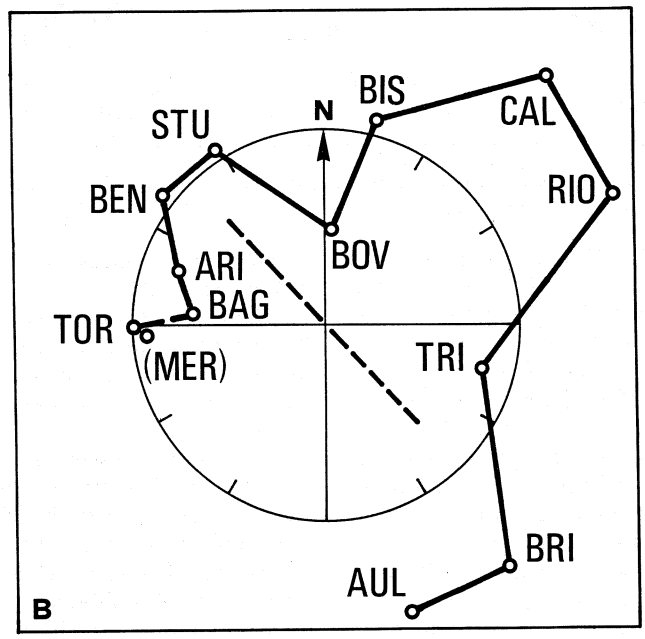

Fig. 6. Radiation pattern of the total horizontal component of *S*-waves from the hypocenter to the stations; focal mechanism: strike 318°, dip 64°, rake 317°. Note the disagreement with fig. 5.

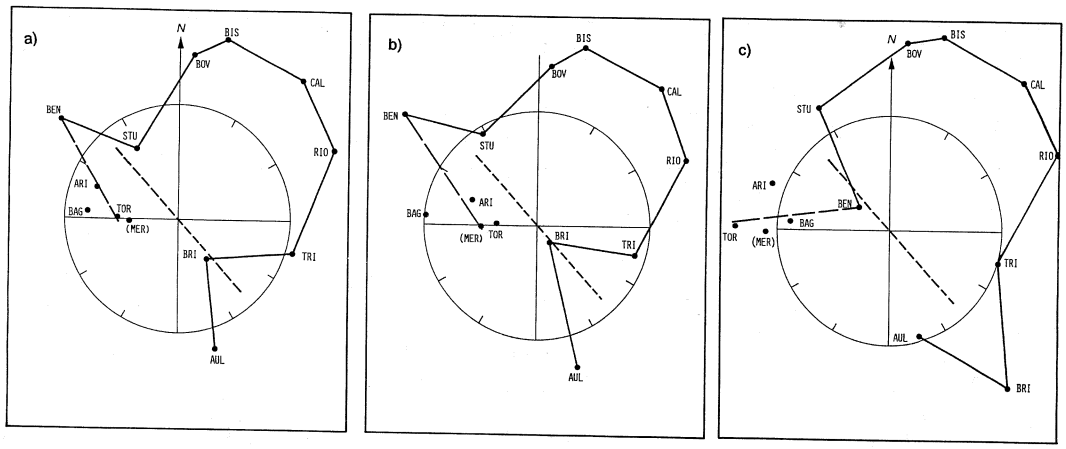

Fig. 7. Radiation pattern of the total horizontal component of *S*-waves from the closest point of the line source of fig. 1 to the stations. In all cases the strike is 318° and the dip 64°. a) Purely normal fault (rake 270°). b) Normal fault with a right-lateral slip component (rake 250°). c) Normal fault with a left-lateral slip component (rake 317°). Note in the last case the agreement with fig. 5.

strong influence of the slip direction on the azimuthal distribution of acceleration.

(After the present analysis was completed we learned (Boore, 1989) that the influence of focal mechanism on strong motion was evidenced also by Vidale (1989) in the case of the Whittier Narrows, California earthquake.)

The known northwestward propagation of the 0s rupture and the likely southeastward propagation of the 19s rupture suggest investigating directivity effects. The data of fig. 5 were further corrected for the radiation pattern dividing them by the total S_H-S_V composed radiation; the results are shown in fig. 8a) and 8b) according to azimuths from the strike of the fault. Since the rupture is bilateral, the stations mostly affected by the rupture of the NW or the SE segments are presented separately. Due to the symmetry of the directivity effect, azimuths to the left of the fault are folded to the right. If we allow for station BAG, fig. 8a) gives a weak indication of a radiation increase in the rupture direction, while in fig. 8b) the maximum at BRI is not supported by sufficient data.

6. The kinematic function

The previous analyses suggest including source dimension, focal mechanism and directivity in a simplified modelling of near-source ground motion.

Let us represent the contribution of every source point to the ground motion at a point P on the surface by the following «kinematic function» (Chiaruttini and Siro, 1991):

$$\mathrm{KF}(P, x) = R(x) / \{D(x) \cdot \cdot [1 - (\Delta V_r / V_S) \cos \vartheta(x)]\} \qquad (2)$$

where R is the radiation pattern of S waves, D is the source-receiver distance, ΔV_r is the rupture velocity variation, V_S is the S-wave velocity, ϑ is the angle between the ray and the direction of rupture propagation, and x is the distance of the source point from the nucleation point.

Expression (2) is valid for a homogeneous elastic medium; dealing with heterogeneous media, $1/D(x)$ should be replaced with the appropriate geometrical spreading. A simple homogeneous model was used here since hypocentral determinations of aftershocks are not improved by adopting a layered medium (Deschamps and King, 1984).

We will show that, apart from a scaling factor to be determined, the maximum value of (2) with x can be used as an estimator of PGA and of macroseismic intensity. We refer to Chiaruttini and Siro (1981) for the problem of correlating intensity with PGA. Consistently with our defini-

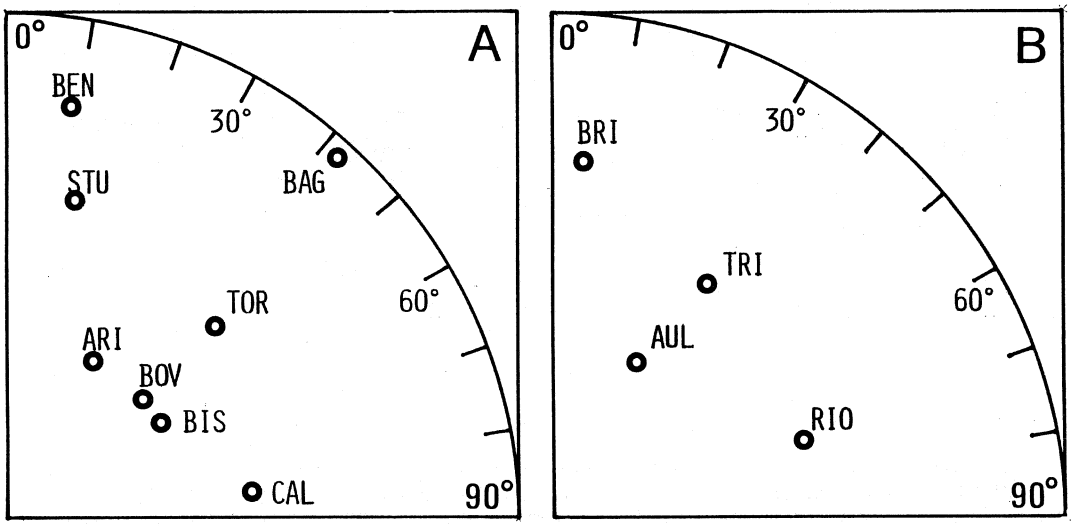

Fig. 8. Recorded PGAs, corrected both for the source distance and for the radiation pattern, plotted as a function of the station azimuth with respect to the epicenter and the fault strike. Azimuths to the left are folded to the right. a) NW segment of the fault. b) SE segment. The cohesionless soil station of MER is not shown in this figure.

tion of PGA, the kinematic function we consider in the following is the composition of the S_H waves and the horizontal component of the S_V waves.

7. Using KF to synthesize the strong-motion field

The event isoseismals are given by Postpischl (1985). Although they have an irregular shape, careful inspection shows that many field observations, often in clusters, are still within the wrong contours. Redrawing the VII and VIII degree isoseismals as in fig. 9 reduces the outliers by some 15 units. Two new sharp intensity minima appear: at Benevento (station BEN) and south of the IX degree area, where station AUL is located. They confirm that the PGA azimuthal minima in these two directions (fig. 5) are not local site effects. Furthermore, the AUL minimum at least is most likely a consequence of the focal mechanism: in fact, the 1694 destructive event produced a similar anomaly in an area some 10 km to the NW, consistent with a shift in the epicentre.

We used the 1980 data to test isoseismals modelling by means of the kinematic function. The maximum of KF for a bilateral rupture (0 and 19s sub-events) was determined for all stations. As a focal mechanism we used the one that best fitted the recorded radiation pattern (strike 318°, dip 64°, rake 317°). Then depth and V_r were adjusted to give the best correlation of PGA with KF. We obtained 5km depth, $V_r = 0.5V_S$, and the following correlation:

$$\log \mathrm{PGA} = -1.161\ (\pm 0.182) + 0.688\ (\pm 0.146) \log \mathrm{KF} \qquad (3)$$

The standard error is 0.18 with a significance of 0.0004, ten times better than any regression of PGA with distance (table I). We therefore conclude that KF is a good predictor for PGA. Also note that the low value of V_r is in agreement with the weak evidence of a directivity effect in fig. 8.

The next step is modeling the macroseismic field. The values of KF were computed over a grid of points and converted to acceleration by (3), obtaining the isolines shown in fig. 10. For easy comparison, the intensity values of fig. 9 were converted to PGA with the relation

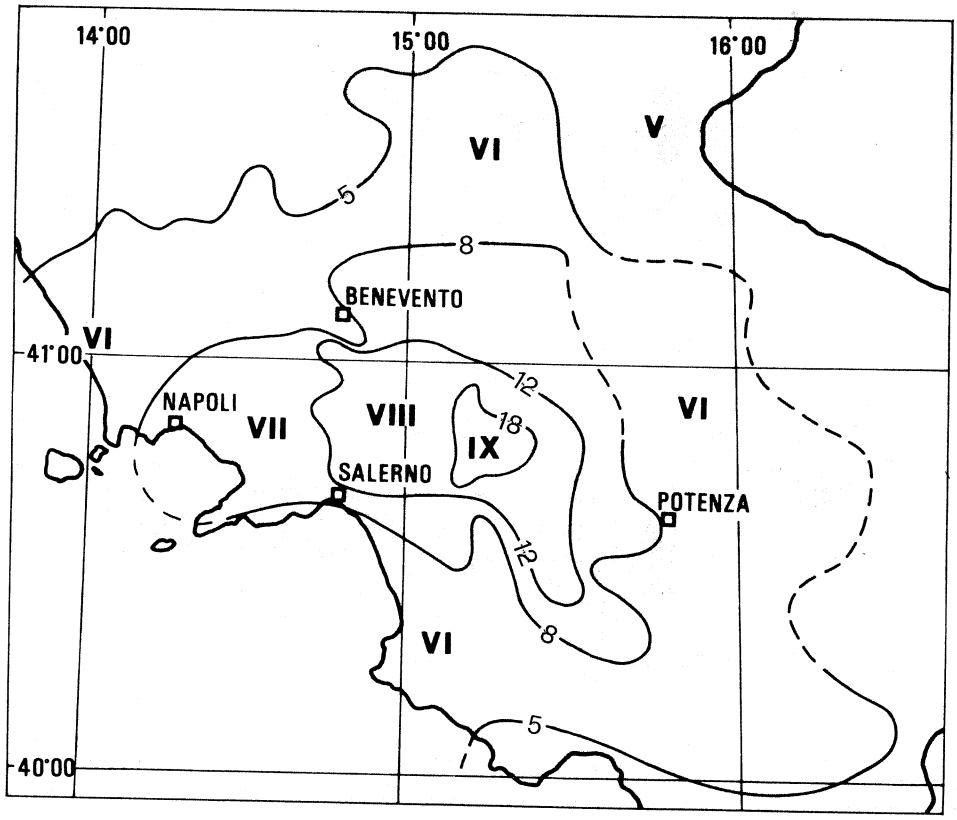

Fig. 9. Observed isoseismals, modified from Postpischl (1985). PGA values are added for comparison with fig. 10.

$$\log \mathrm{PGA} = -0.42 + 0.19\ (\pm 0.05)\ I_{\mathrm{MCS}} \quad (4)$$

with a standard error of 0.33, determined from the 21 acceleration values of all stations triggered by this earthquake.

Before comparing observed and synthetic isoseismals, let us recall that field macroseismic intensity accounts for the effect of the whole earthquake, the 39s sub-event included. Accelerograms show that this third episode radiated mostly towards NE causing the recorded maximum at station CAL. Therefore,we expect that our model is able to include the most damaging effects in all directions, with the plausible exception of the NE sector. A comparison of synthetic and observed isolines shows several common features: the lengthening towards SE, a sharp amplitude decrease towards SSW, and lobes toward the city of Salerno towards NE and NNE. There is also quantitative agreement between the acceleration values in fig. 9 and 10. The major discrepancy is in the NW direction, possibly because our source extends too far in that direction or because a different rupture geometry is active there, such as the fault rotation to the north suggested by Bernard and Zollo (1989). Obviously, the resemblance between observed and synthetic isolines is poor at very short distances from the assumed line source.

8. Concluding remarks

The analysis of *S*-wave polarizations evidenced some details about energy radiation of a complex earthquake. The first and strongest of

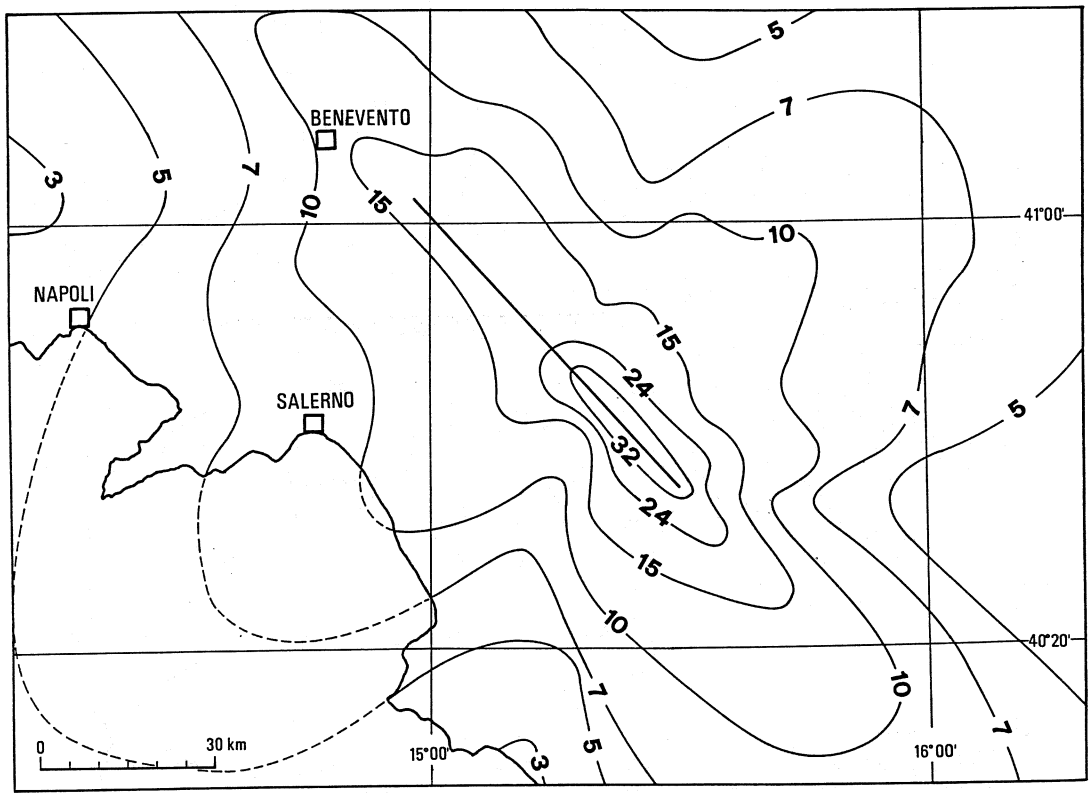

Fig. 10. Synthetic isoseismals of the November 23 earthquake obtained by means of the kinematic function. The curves are quoted in units of PGA (*g*/100).

the three main sub-events had a clear unilateral rupture propagation from the epicentre to the NW. At stations within a few tens of kilometres from the source, the recorded PGAs originated from the closest source segments. It also appears that the broken parts of the fault continued to radiate a few seconds after the passage of the rupture front.

After correction for the source-receiver distance, the wave amplitudes show a smooth variation with azimuth controlled by the source geometry: spatial extension and focal mechanism. The effect of the directivity is limited as a consequence of a low rupture propagation.

A kinematic function was introduced that takes into account the basic source parameters: size, focal mechanism, rupture velocity. It proves to be a good predictor of the PGA. The kinematic function was also used to model the macroseismic field of the earthquake, obtaining synthetic isoseismals that reasonably resemble the observed ones. Owing to its simplicity, the KF is mainly suited to the study of historical earthquakes for which sophisticated modelling is hardly justified by the scarcity of the data. Another possible application could be when a fast – even if rough – prediction of isoseismals is needed, as in planning initial rescues after a destructive 'quake when direct information about damage is not available from the stricken area.

(*) Previously: L. Siro. Recently, the author has reassumed the original family name that had been changed in 1928.

REFERENCES

BERNARD, P. and A. ZOLLO (1989): The Irpinia (Italy) 1980 earthquake: detailed analysis of a complex normal fault, *J. Geophys. Res.*, **94**, 1631-1647.

BOORE, D.M. (1989): private communication.

BRÜSTLE, W. and G. MÜLLER (1983): Moment and duration of shallow earthquakes from Love wave modeling for regional distances, *Phys. Earth Planet. Inter.*, **32**, 312-324.

CHIARUTTINI, C. and L. SIRO (1981): Attendibilità delle correlazioni accelerazione-intensità, in *Atti Conv. P. F. Geodinamica, Udine, Italia, Rend. Soc. Geol. It.*, **4**, 655-658.

CHIARUTTINI, C. and L. SIRO (1991): Focal mechanism of an earthquake of Baroque age in the «Regno delle Due Sicilie» (southern Italy), in *Proc. XIII Gen. Ass. EGS., Tectonophysics*, **193**, 195-203.

DESCHAMPS, A. and G.C.P. KING (1983): The Campania-Lucania (Southern Italy) earthquake of 23 November 1980, *Earth Planet. Sci. Lett.*, **62**, 296-304.

DESCHAMPS, A. and G.C.P. KING (1984): Aftershocks of the Campania-Lucania (Italy) earthquake of 23 November 1980, *Bull. Seismol. Soc. Am.*, **74**, 6, 2483-2517.

FAITELLI, G.M. (1978): *Studio geologico delle aree sulle quali ricadono le postazioni accelerometriche della rete di rilevamento sismico dell'ENEL. ENEL Direzione delle costruzioni.* Unprinted Technical Report, Roma, Italia.

NUTTLI, O. and J.D. WHITMORE (1962): On the determination of the polarization angle of the *S*-wave, *Bull. Seismol. Soc. Am.*, **52**, 1, 95-107.

PANTOSTI, D. and G. VALENSISE (1990): Fault mechanism and complexity of the November 23, 1980, Campania-Lucania earthquake, inferred from surface observations, *J. Geophys. Res..*, **95**, B10, 15319-15241.

POSTPISCHL, D. (Editor) (1985): Atlas of isoseismal maps of Italian earthquakes, *Quad. Ric. Sci.* (CNR, Bologna, Italia), n. 114, vol. 2a.

SCARPA, R. and D. SLEJKO (1982): Some analyses of seismological data, in *Southern Italy November 23 1980 Earthquake*, The Italian Geodynamics Project of CNR, Publ. n. 503, Roma.

SIRO, L. and C. CHIARUTTINI (1989): Source complexity of the 1980 Southern Italian earthquake from the analysis of strong-motion *S*-wave polarization, *Bull. Seismol. Soc. Am.*, **79**, 6, 1810-1832

SIRO, L. and C. CHIARUTTINI (1991): Reply to P. Bernard and A. Zollo's «Comment on Source complexity of the 1980 Southern Italian earthquake from the analysis of strong-motion *S*-wave polarization», *Bull. Seismol. Soc. Am.*, **81**, 1, 282- 288.

VIDALE, J.E. (1989): Influence of focal mechanism on peak accelerations of strong motions of the Whittier Narrows earthquake and an aftershock, *J. Geophys. Res.*, **94**, B7, 9607-9613.

WESTAWAY, R. and J. JACKSON (1987): The earthquake of November 23 in Campania-Basilicata (southern Italy), *Geophys. J. R. Astron. Soc.*, **90**, 375-443.